

# Broadly, independent-tunable, dual-wavelength mid-infrared ultrafast optical parametric oscillator

Yuwei Jin,<sup>1</sup> Simona M. Cristescu,<sup>1</sup> Frans J. M. Harren,<sup>1</sup> and Julien Mandon<sup>1, a)</sup>

*Molecular and Laser Physics, Institute for Molecules and Materials,  
Radboud University, P.O. Box 9010, 6500 GL Nijmegen,  
The Netherlands*

(Dated: 13 August 2015)

## Abstract

We demonstrate a two-crystal mid-infrared dual-wavelength optical parametric oscillator, synchronously pumped by a high power femtosecond Yb:fiber laser. The singly-resonant ring cavity, containing two periodically poled lithium niobate crystals, is capable of generating two synchronized idler wavelengths, independently tunable over 30 THz in the 2.9 - 4.2  $\mu\text{m}$  wavelength region, due to the cascaded quadratic nonlinear effect. The independent tunability of the two idlers makes the optical parametric oscillator a promising source for ultrafast pulse generation towards the THz wavelength region, based on different frequency generation. In addition, the observed frequency doubled idler within the crystal indicates the possibility to realize a broadband optical self-phase locking between pump, signal, idler and higher order generated parametric lights.

---

<sup>a)</sup>j.mandon@science.ru.nl;

<http://www.ru.nl/tracegasfacility/>

## I. INTRODUCTION

Dual-wavelength operation within a single laser cavity is promising for a variety of applications such as coherent pulse synthesis, THz generation, pump-probe experiments and CARS<sup>1-4</sup>. For conventional solid-state ultrafast lasers, dual-wavelength operations were observed and demonstrated with Ti:sapphire lasers at 800 nm<sup>5,6</sup> and Tm:CaYAlO<sub>4</sub> lasers at 2  $\mu\text{m}$ <sup>7</sup>. Besides, dual-wavelength operation was also realized with a *Q*-switched cascade fiber laser at 3  $\mu\text{m}$ <sup>8</sup>. Optical parametric oscillators (OPOs) are well-established mid-infrared sources offering coherent light, high power, broad bandwidth and broad tuning range. Nowadays, OPOs are also widely used for a variety of applications such as mid-infrared frequency comb generation and spectroscopy<sup>9-11</sup>. Specifically, synchronously pumped OPOs offer an new opportunity for synchronized pulses generation at two different wavelength regions<sup>12-19</sup>, that can be directly used for THz generation based on different frequency generation (DFG)<sup>20-24</sup>. In the case of an OPO with a single cavity, the dual-wavelength operation is realized when the two resonant pulse trains have the same round trip time delay<sup>12</sup>. In literature, the simultaneous dual-wavelength operation is explained by the balance between phase matching and group-velocity mismatching between the two resonant pulses<sup>14,16</sup>. Experimental results also indicate a stable relative carrier-envelope phase-slip frequencies within a dual-wavelength femtosecond OPO, which is of great interest for various applications such as quantum control and coherent pulse synthesis<sup>13</sup>. However, most dual-wavelength OPOs reported provide limited dual-wavelength tunability and broadband arbitrary wavelength tuning of the two idlers is not possible.

In this paper, we present the experimental observation of dual-wavelength operation within a two-crystal OPO pumped by a femtosecond Yb:fiber laser. By tuning the cavity length, the simultaneous dual-wavelength operation is realized when the two crystals are at different poling periods. To our knowledge, this is the first demonstration of an independently-tunable, synchronously-pumped, dual-wavelength, ultrafast OPO generating arbitrarily tunable idlers across a 30 THz spectral region between 2.9  $\mu\text{m}$  and 4.2  $\mu\text{m}$ . To characterize the OPO, we have also observed the behavior of several cascaded parametric processes within the nonlinear crystals, such as the second harmonic generation(SHG) of the idler, indicating the possibility to achieve optical self-phase locking between pump, signal and idler when the spectrum of the frequency doubled idler overlaps the spectrum of the

signal. It is worth mentioning that previously, self-phase locking of continuous-wave (CW) OPOs has been achieved by using the intra-cavity frequency-doubled idler<sup>25–28</sup>.

## II. DUAL-WAVELENGTH OPERATION OF THE OPTICAL PARAMETRIC OSCILLATOR

The experimental setup of the synchronously pumped singly-resonant OPO is similar to the one described previously<sup>11,29</sup>. As illustrated in Fig. 1, the difference is that the two crystals (both temperatures are stabilized at 80 degree) are pumped by a single femtosecond Yb-fiber laser instead of two similar pump lasers in order to have exactly the same repetition rates of the pump pulses for the crystals. The two generated idlers are recombined together with a mid-infrared beam splitter (BS 2), coupling to a commercial Fourier transform spectrometer (FTS) for characterization. The two resonating signals are counter-propagating in the ring cavity and do not interact with one another within the crystals. The zero dispersion wavelength of the cavity is calculated to be at 1532 nm (195.7 THz), considering both the crystal dispersion<sup>30</sup> and the six chirped mirrors.

To measure the output spectra of the OPO, the poling period of one crystal is fixed at

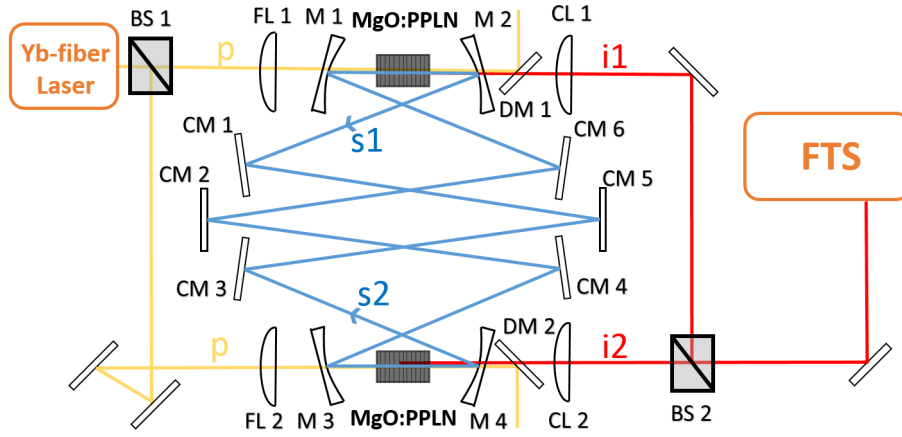


FIG. 1. Scheme of the femtosecond laser pumped dual-wavelength OPO. p, s1-s2, i1-i2, pump, signals, and idlers, respectively. BS1-BS2, beam splitters. FL1-FL2, focusing lenses ( $f = 100$  mm). M1-M4, curved mirrors ( $R = 100$  mm). CM1-CM6, chirped mirrors. DM1-DM2, dichroic mirrors. CL1-CL2, collimating lenses ( $f = 100$  mm). FTS, Fourier transform spectrometer. One moving stage is mounted on CM 5 (not shown).

31.02  $\mu\text{m}$ , while the poling period of the second crystal is tuned from 27.91  $\mu\text{m}$  to 30.49  $\mu\text{m}$ . Figure 2(a) shows the measured spectrum when only one crystal with a 31.02  $\mu\text{m}$  poling period is directly pumped by the femtosecond laser. When the two crystals are pumped by the femtosecond laser, two idlers are generated simultaneously within the two crystals at different wavelengths. It can be noticed that the first idler is not spectrally affected when both crystals are pumped. By changing the poling period of the second crystal, dual-wavelength operation across a 30 THz spectral region between 2.9 - 4.2  $\mu\text{m}$  is realized (Fig. 2(b) - 2(h)). The two idler wavelengths are operating independently and as such can be tuned to arbitrary wavelength regions.

The behavior of the dual-wavelength operation is cavity length dependent. Measurements have been done when the poling periods of the two crystals are set to be 28.28 and 29.52  $\mu\text{m}$ . As illustrated in Fig. 3, by tuning the cavity length, both the single-wavelength and the dual-wavelength operations are achieved when the pump power is 1.1 W. Figures 3(b), 3(e) and 3(h) exhibit the signal spectrum, the idler spectrum and the interferogram of the idler retrieved from the FTS, respectively, for which a relative cavity length  $\Delta L = 0 \mu\text{m}$  is assumed (i.e. the cavity length that is synchronized to the repetition frequency of the pump

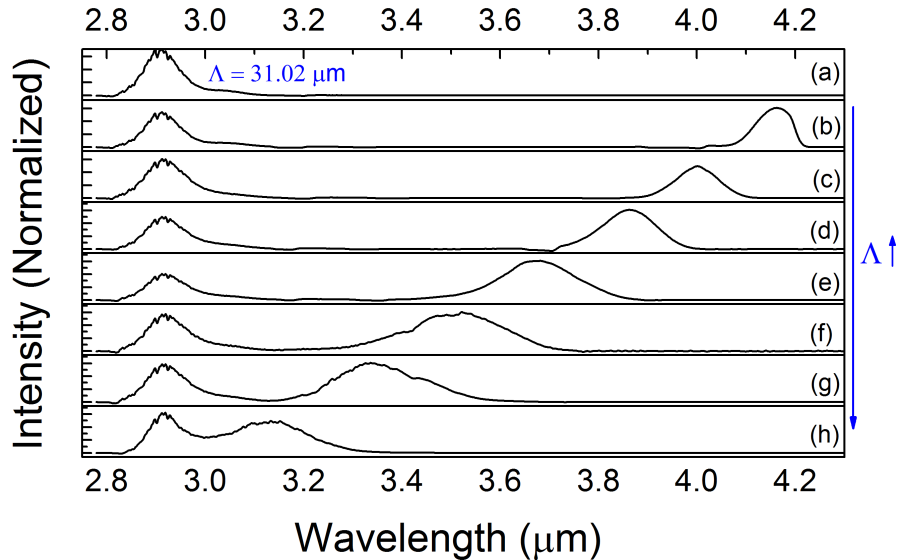


FIG. 2. Panel (a): Generated idler light with one crystal pumped. Panel (b)-(h): Generated idler light with two crystals pumped, in which the poling period of the second crystal is varied between 27.91 - 30.49  $\mu\text{m}$ . Spectra are measured by the FTS.

laser). Moreover, each OPO could deliver pulses singly at either wavelength by detuning the cavity length as can be seen in Fig. 3(a), 3(d), 3(g) and Fig. 3(c), 3(f), 3(i). The reason the relative intensities of the signals are quite weak is the usage of the high-reflectivity mirrors of the OPO cavity.

### III. CHARACTERIZATION OF THE OPTICAL PARAMETRIC OSCILLATOR

It is worth noticing that the arbitrary wavelength tuning of a dual-wavelength OPO within a single cavity cannot be explained from the conventional perspective<sup>12,14,16</sup>, hence, more experiments have been done to have an in-depth characterization of the OPO. As the two resonating signals are counter-propagating in the ring cavity and do not interact with one another, the beam splitter (BS 1 in Fig. 1) can be removed to characterize the two OPOs separately. Therefore, only one crystal is pumped directly by the Yb-fiber laser. From the output of the OPO, idler in the mid-infrared, signal and frequency doubled idler in the near infrared can be observed simultaneously by using a FTS. In addition, other cascaded parametric lights below  $1\text{ }\mu\text{m}$  can be monitored by a visible light spectrometer. Power

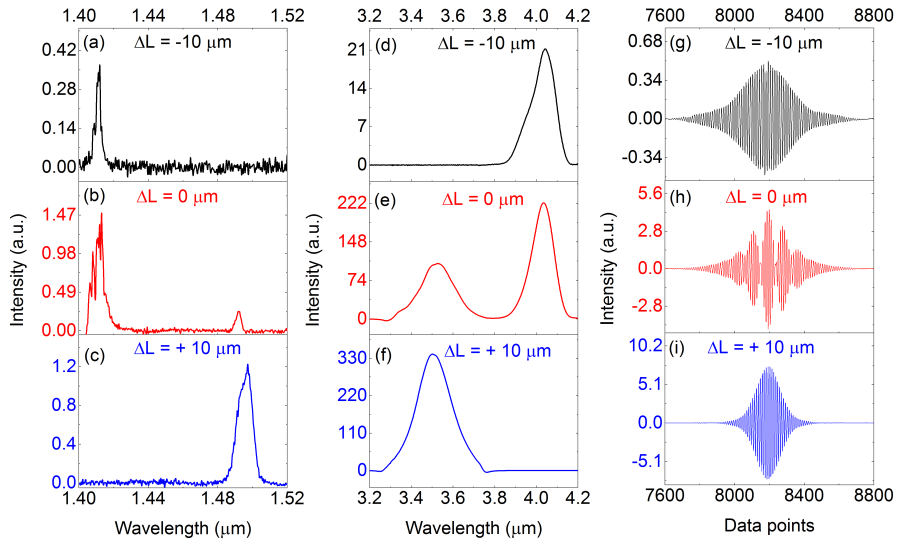


FIG. 3. Panel (a)-(c): Measured signal spectra by tuning the cavity length. Panel (d)-(f): Measured idler spectra by tuning the cavity length. Panel (g)-(i): Corresponding interferograms of idlers retrieved from the FTS by tuning the cavity length.

scaling measurements are performed when the poling periods of the two crystals are set to be  $29.08 \mu\text{m}$ . As illustrated in Fig. 4(a), the spectra of signals between  $1.4$  and  $1.7 \mu\text{m}$  and the spectra of frequency doubled idlers between  $1.8$  and  $1.9 \mu\text{m}$  are recorded. The corresponding idler spectra between  $3.2$  and  $4.1 \mu\text{m}$  are also shown in Fig. 4(b). A spectral broadening effect is observed while increasing the pump power. At a  $1.7 \text{ W}$  average pump power, the signal covers a  $300 \text{ nm}$  spectral range corresponding to a  $1000 \text{ cm}^{-1}$  ( $30 \text{ THz}$ ) bandwidth, revealing a modulated multi-peak structure. Both the spectral broadening effect and the modulated multi-peak structure indicate the presence of a nonlinear phase modulation, which is plausibly due to the cascaded quadratic nonlinearity for the signal that is treated as the fundamental wave in this case<sup>31</sup>. These cascaded quadratic processes have been shown to resemble a  $\chi^{(3)}$  process<sup>32–36</sup>, and the most common cascaded quadratic effect involves a single-step process, such as non-phase-matched SHG in a dispersive quadratic media. Meanwhile, cascaded quadratic processes due to third-harmonic generation (THG) have also been discussed previously<sup>37–39</sup>.

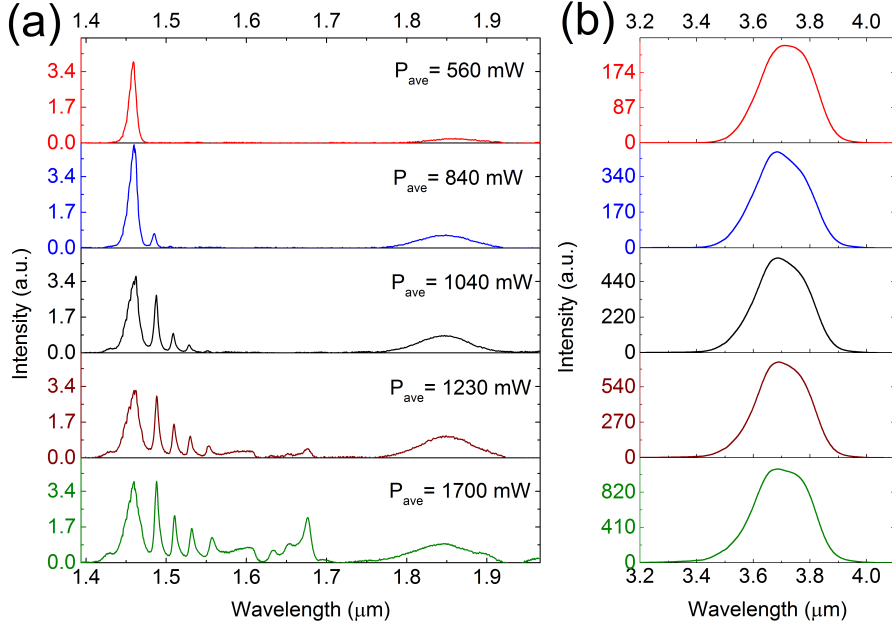


FIG. 4. Panel (a): Recorded spectra between  $1.3$  and  $2.0 \mu\text{m}$  under different pump powers. The peaks between  $1.8$  and  $1.9 \mu\text{m}$  are the frequency doubled idlers. The lights between  $1.4$  and  $1.7 \mu\text{m}$  are recorded signals. Panel (b): The corresponding idler spectra between  $3.2$  and  $4.1 \mu\text{m}$  under different pump powers.

To further confirm the presence of the cascaded quadratic processes, a series of measurements are performed with a 1.7 W pump power. By tuning the poling periods of two crystals from 27.91 to 31.02  $\mu\text{m}$ , spectra between 400 and 800 nm (375 to 749 THz) are recorded. In these measurements, both the THG and SHG of the signal are observed as demonstrated in gray sections (1) and (2) within Fig. 5(a), respectively. In this case, both the phase-mismatching for SHG and THG of the signal can be calculated by the following formulae  $\Delta k_1 = 2\pi(\lambda_{2s}/n_{2s} - 2\lambda_s/n_s - 1/\Lambda)$  and  $\Delta k_2 = 2\pi(\lambda_{3s}/n_{3s} - 3\lambda_s/n_s - 1/\Lambda)$ , respectively, where  $\lambda_s$ ,  $\lambda_{2s}$ ,  $\lambda_{3s}$  are the wavelengths of the signal, the SHG of the signal, and the THG of the signal;  $n_s$ ,  $n_{2s}$ ,  $n_{3s}$  are corresponding refractive indices;  $\Lambda$  represents poling period of the crystal. Figure 5(b) and 5(c) give an example of the results upon these calculations, assuming that the poling period is 29.08  $\mu\text{m}$ . The observation of both non-phase-matched SHG and THG of the resonating signal implies the presence of cascaded quadratic processes which we believe contribute to the dual-wavelength operation.

When the poling period of the pumped crystal is 30.49  $\mu\text{m}$  with a 300 mW average pump power, a spectrum of the cascaded parametric lights generated from the OPO along with the

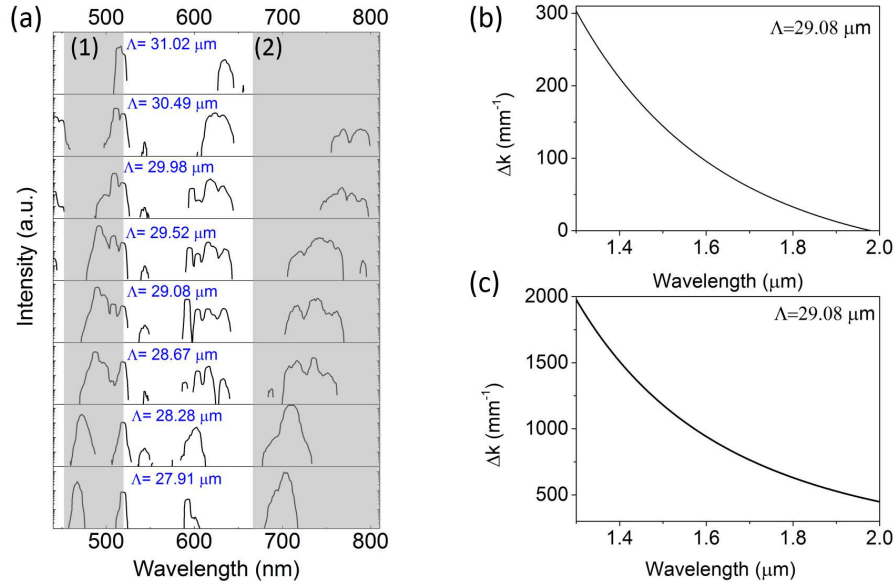


FIG. 5. Panel (a): Recorded spectra between 400 and 800 nm for different poling periods of the PPLN crystal. All vertical axes are at logarithmic scales. Panel (b): Phase mismatch of SHG when the fundamental wave is at different wavelength between 1.3 and 2.0  $\mu\text{m}$ . Panel (c): Phase mismatch of THG when the fundamental wave is at different wavelength between 1.3 and 2.0  $\mu\text{m}$ .

residual pump light ( $p$ ), leaked signal light ( $s$ ) from the cavity, and the generated idler light ( $i$ ), are recorded with an optical spectrum analyzer (OSA). As illustrated in Fig. 6(a), the dominating, nonlinearly generated intensities are: the sum frequencies of pump and signal ( $p+s$ ), pump and idler, and doubling frequency of pump ( $2p$ ), next to other frequencies ( $2s$ ,  $3s$ ,  $p+2s$ ,  $2p+i$ ,  $2p+s$ ). By monitoring the light leaking from mirror CM3 by using a fast visible light detector, two beating frequencies are observed centered on half the repetition frequency (45 MHz) of the pump laser (Fig. 6(b)). This beating frequency originates from the overlap between different generated parametric lights as shown in the gray sections in Fig. 6(a). Assume that the frequencies of the pump and the idler are  $f_p$  and  $f_i$ , the beating frequencies observed at the three gray sections are  $f_{2p+i} - f_{p+2s}$ ,  $f_{3s} - f_{2p}$ , and  $f_{2s} - f_{p+i}$ , respectively. The value of these beating frequencies are all equal to  $f_p - 3f_i$ , considering that  $f_p = f_s + f_i$ . Moreover, the same beating frequency in the mid-infrared wavelength region is also observed by using a fast infrared detector (Vigo, PVI-4TE, 50 MHz bandwidth) at the output of the OPO after a Germanium collimating lens.

To explain the observed beating frequencies both in the mid-infrared and visible regions, the parametric processes within the OPO are illustrated in Fig. 7(a). Firstly, the pump wavelength ( $f_p$ ) is divided into a signal wavelength ( $f_s$ ) and an idler wavelength ( $f_i$ ). The SHG of the idler is at  $2f_i$  while the different frequency generation (DFG) between the

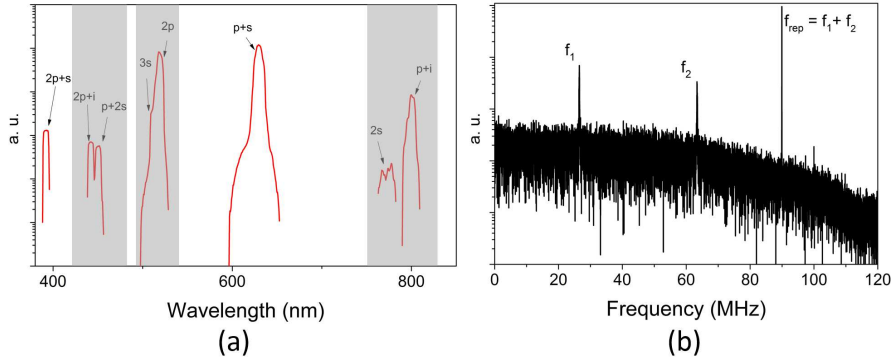


FIG. 6. Panel (a): Recorded spectrum of the cascaded parametric light generated from the OPO along with the residual pump( $p$ ), leaked signal( $s$ ) and generated idler( $i$ ). Within the grey sections, there are overlaps between the different cascaded parametric lights, at some poling periods. Panel (b): Beating signal (log scale) detected by using a single visible light detector,  $f_1 = f_p - 3f_i$  or  $f_2 = f_p - 3f_i$ . All vertical axes are at logarithmic scales.



frequency doubled idler ( $2f_i$ ) and the pump ( $f_p$ ) is at  $f_p - 2f_i$ . By changing the poling periods in the crystal at  $27.91 \mu\text{m}$ ,  $28.28 \mu\text{m}$  and  $29.52 \mu\text{m}$ , the frequency doubled idler ( $2f_i$ ) and the signal ( $f_s$ ) start to merge as can be seen in Fig. 7(b), generating a beating frequency at  $f_p - 3f_i$ . Figure 7(c) illustrates the merging of the THG of the signal ( $3f_s$ ) with the SHG of the pump ( $2f_p$ ), also generating a beating frequency at  $f_p - 3f_i$ . In addition, the beating frequency detected in the mid-infrared is calculated to be  $f_{p-2i} - f_i = f_p - 2f_i - f_i = f_p - 3f_i$ , which is the same value when compared to the beating frequencies both in the near infrared and the visible wavelength region. It is expected that from the overlap between the signal and the frequency doubled idler (Fig. 7(a)), self-phase locking can be achieved from this

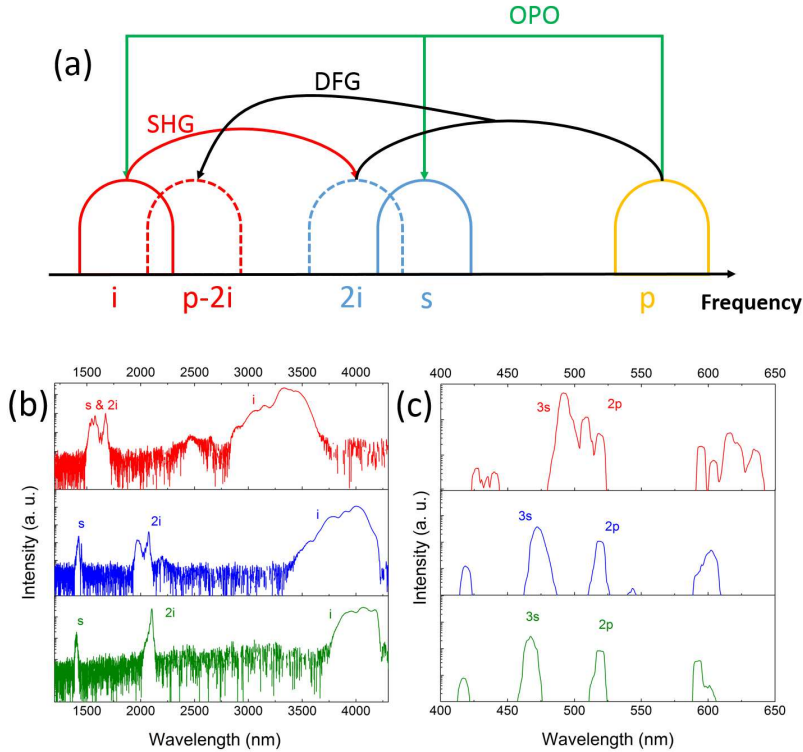


FIG. 7. Panel (a): Parametric processes within the OPO cavity. OPO: optical parametric oscillation; DFG: different frequency generation; SHG: second harmonic generation. p,s,and i: pump, signal and idler. Panel (b): Spectra measured between 1000 nm and 5000 nm (60 to 300 THz) at three different poling periods, indicating the merging between the signal ( $s$ ) and the second harmonic of idler ( $2i$ ). Panel (c): Spectra measured between 400 nm and 650 nm (461 to 749 THz) at the three different poling periods, indicating the merging between the third harmonic of signal ( $3s$ ) and the second harmonic of pump ( $2p$ ). All vertical axes are at logarithmic scales.

TABLE I. The corresponding frequencies of different cascaded parametric lights when the OPO would be self-phase locked between the frequency doubled idler and the signal.  $f_i$  is the idler frequency.

Parametric lights Frequencies		Parametric lights Frequencies	
$i$ and $p - 2i$	$f_i$	$p + s$	$5f_i$
$s$ and $2i$	$2f_i$	$3s$ and $2p$	$6f_i$
$p$	$3f_i$	$2p + i$ and $p + 2s$	$7f_i$
$2s$ and $p + i$	$4f_i$	$2p + s$	$8f_i$

femtosecond laser pumped OPO, and that all generated parametric lights can be optically phase locked to the pump source. One way to establish this is by stabilizing the cavity length with a feedback loop<sup>40</sup>. Once the self-phase locking is realized,  $f_p$  is constantly equal to  $3f_i$ , and one can achieve phase coherent generation at frequencies of  $N \cdot f_i (N = 1 - 8)$  from a single OPO laser source, simultaneously, which are illustrated in Table 1.

#### IV. DISCUSSION AND CONCLUSION

For a femtosecond OPO with a single gain medium, pumped at a fixed repetition frequency, the central wavelength of the signal wave shifts by changing the cavity length, maintaining the round trip time delay corresponding to the fixed cavity length<sup>14,29</sup>. Asynchronous pumping can also be achieved at a fixed cavity length by using two femtosecond lasers with different repetition frequencies<sup>29,41</sup>. In this case, two pulse trains (signal) at different central wavelengths maintain the same round trip time delay due to the difference of group velocities within the crystal. Conventionally, dual-wavelength operation within a single cavity at one repetition frequency can be realized when the two resonant pulse trains have the same round trip time delay, implying that the tuning of the two wavelengths is strongly correlated and not arbitrary<sup>12,14,16</sup>. In this work, the two-crystal OPO offers arbitrary dual-wavelength generation, due to the use of different poling periods in the crystals offering different gain bandwidths. Next to this, the OPO is singly-resonant on the signal without output coupler, reserving extremely high signal power within the cavity. This two crystal OPO cavity is capable of generating two synchronized idler beams that are independently tunable across a 30 THz spectral region between 2.9 - 4.2  $\mu\text{m}$ . The independent tunability of

the two idlers can be explained by taking higher order nonlinear effects into account, such as the cascaded quadratic nonlinearity. These cascaded processes in quadratic media induce a nonlinear phase shift on the fundamental wave by back-conversion of the phase-mismatched second harmonic wave, which is equivalent to third-order nonlinearity<sup>32,33,42,43</sup>. In practice, active group velocity control within a PPLN crystal has already been achieved based on the cascaded quadratic nonlinearity<sup>43,44</sup>. We believe that the group velocity mismatch between the two wavelengths are compensated by the nonlinear phase shift, due to the cascaded quadratic nonlinearities that is analogous to the third-order nonlinearity in a conventional mode-locked laser in the case of Kerr modulation<sup>33,45</sup>.

In conclusion, for the first time, we have experimentally demonstrated dual-wavelength operation within a two-crystal OPO cavity, generating two broadband idler beams that are independently tunable across a 30 THz spectral range between 2.9 - 4.2  $\mu\text{m}$ . Such passively synchronized dual-wavelength pulses could be coupled to a nonlinear crystal, such as OP-GaAs<sup>22</sup>, to generate light from the far-infrared to THz wavelength region based on the different frequency generation. Besides, the spatially separated pulses are also ideal sources for mid-infrared pump-probe experiments. To characterize the OPO, we have observed second harmonic generation of the idler ( $2i$ ) directly, without using a tandem crystal. The observed merging effect between the signal and the frequency doubled idler indicates a possibility to realize self-phase locking between them.

## ACKNOWLEDGMENTS

This work is financially supported by the Technology Foundation STW, under project number 11830.

## REFERENCES

- <sup>1</sup>L. -S. Ma, R. K. Shelton, H. C. Kapteyu, M. M. Murnane, and J. Ye, “Sub-10-femtosecond active synchronization of two passively mode-locked Ti:sapphire oscillators,” *Phys. Rev. A* **64**, 021802 (2001).
- <sup>2</sup>K. Kawase, T. Hatanaka, H. Takahashi, K. Nakamura, T. Taniuchi, and H. Ito, “Tunable terahertz-wave generation from DAST crystal by dual signal-wave parametric oscillation of periodically poled lithium niobate,” *Opt. Lett.* **25**, 1714–1716 (2000).
- <sup>3</sup>A. Yu, X. Ye, D. Ionascu, W. Cao, and P. M. Champion, “Two-color pump-probe laser spectroscopy instrument with picosecond time-resolved electronic delay and extended scan range,” *Rev. Sci. Instrum.* **76**, 114301 (2005).
- <sup>4</sup>F. Ganikhanov, S. Carrasco, X. S. Xie, M. Katz, W. Seitz, and D. Kopf, “Broadly tunable dual-wavelength light source for coherent anti-Stokes Raman scattering microscopy,” *Opt. Lett.* **31**, 1292–1294 (2006).
- <sup>5</sup>M. R. X. de Barros, and P. C. Becker, “Two-color synchronously mode-locked femtosecond Ti:sapphire laser,” *Opt. Lett.* **18**, 631–633 (1993).
- <sup>6</sup>Z. Zhang, and T. Yagi, “Dual-wavelength synchronous operation of a mode-locked Ti:sapphire laser based on self-spectrum splitting,” *Opt. Lett.* **18**, 2126–2128 (1993).
- <sup>7</sup>L. C. Kong, Z. P. Qin, G. Q. Xie, X. D. Xu, J. Xu, P. Yuan, and L. J. Qian, “Dual-wavelength synchronous operation of a mode-locked 2- $\mu\text{m}$  Tm:CaYAlO<sub>4</sub> laser,” *Opt. Lett.* **40**, 356–358 (2015).
- <sup>8</sup>J. Li, T. Hu, and S. D. Jackson, “Dual-wavelength *Q*-switched cascade laser,” *Opt. Lett.* **37**, 2208–2210 (2012).
- <sup>9</sup>F. Adler, K. C. Cossel, M. J. Thorpe, I. Hartl, M. E. Fermann, and J. Ye, “Phase-stabilized, 1.5 W frequency comb at 2.8-4.8  $\mu\text{m}$ ,” *Opt. Lett.* **34**, 1330–1332 (2009).
- <sup>10</sup>A. Foltynowicz, T. Ban, P. Masłowski, F. Adler, and J. Ye, “Quantum-Noise-Limited Optical Frequency Comb Spectroscopy,” *Phys. Rev. Lett.* **107**, 233002 (2011).
- <sup>11</sup>Y. Jin, S. M. Cristescu, F. J. M. Harren and J. Mandon, “Two-crystal mid-infrared optical parametric oscillator for absorption and dispersion dual-comb spectroscopy,” *Opt. Lett.* **39**, 3270–3273 (2014).
- <sup>12</sup>K. C. Burr, C. L. Tang, M. A. Arbore, and M. M. Fejer, “High-repetition-rate femtosecond optical parametric oscillator based on periodically poled lithium niobate,” *Appl. Phys.*

- Lett. **70** (25), 3341–3343 (1997).
- <sup>13</sup>J. Sun, B. J. S. Gale, and D. T. Reid, “Dual-color operation of a femtosecond optical parametric oscillator exhibiting stable relative carrier-envelope phase-slip frequency,” Opt. Lett. **31**, 2021–2023 (2006).
  - <sup>14</sup>L. Tartara, “Simple and versatile dual-signal wave optical parametric oscillator,” Opt. Lett. **32**, 1105–1107 (2007).
  - <sup>15</sup>G. K. Samanta, and M. Ebrahim-Zadeh, “Dual-wavelength, two-crystal, continuous-wave optical parametric oscillator,” Opt. Lett. **36**, 3033–3035 (2011).
  - <sup>16</sup>L. Xu, X. Zhong, J. Zhu, H. Han, and Z. Wei, “Efficient femtosecond optical parametric oscillator with dual-wavelength operation,” Opt. Lett. **37**, 1436–1438 (2012).
  - <sup>17</sup>P. Jiang, T. Chen, D. Yang, B. Wu, S. Cai, and Y. Shen, “A fiber laser pumped dual-wavelength mid-infrared optical parametric oscillator based on aperiodically poled magnesium oxide doped lithium niobate,” Laser Phys. Lett. **10**, 115405 (2013).
  - <sup>18</sup>V. Ramaiah-Badarla, S. C. Kumar, and M. Ebrahim-Zadeh, “Fiber-laser-pumped, dual-wavelength, picosecond optical parametric oscillator,” Opt. Lett. **39**, 2739–2742 (2014).
  - <sup>19</sup>C. Gu, M. Hu, J. Fan, Y. Song, B. Liu, C. Wang, “High-power, dual-wavelength femtosecond  $\text{LiB}_3\text{O}_5$  optical parametric oscillator pumped by fiber laser,” Opt. Lett. **39**, 3896–3899 (2014).
  - <sup>20</sup>T. Taniuchi, and H. Nakanishi, “Collinear phase-matched terahertz-wave generation in GaP crystal using a dual-wavelength optical parametric oscillator,” J. Appl. Phys. **95**, 7588 (2004).
  - <sup>21</sup>J. E. Schaar, K. L. Vodopyanov, and M. M. Fejer, “Intracavity terahertz-wave generation in a synchronously pumped optical parametric oscillator using quasi-phase-matched GaAs,” Opt. Lett. **32**, 1284–1286 (2007).
  - <sup>22</sup>K. L. Vodopyanov, “Optical THz-wave generation with periodically-inverted GaAs,” Laser & Photon. Rev. **2** (1-2), 11–25 (2008).
  - <sup>23</sup>K. L. Vodopyanov, W. C. Hurlbut, and V. G. Kozlov, “Photonic THz generation in GaAs via resonantly enhanced intracavity multispectral mixing,” Appl. Phys. Lett. **99**, 041104 (2011).
  - <sup>24</sup>R. Hegenbarth, A. Steinmann, S. Sarkisov, and H. Giessen, “Milliwatt-level mid-infrared (10.5–16.5  $\mu\text{m}$ ) difference frequency generation with a femtosecond dual-signal-wavelength optical parametric oscillator,” Opt. Lett. **37**, 3513–3515 (2012).

- <sup>25</sup>D.-H. Lee, M. E. Klein, J.-P. Meyn, P. Groß, R. Wallenstein, and K.-J. Boller, “Self-injection-locking of a CW-OPO by intracavity frequency-doubling the idler wave,” *Opt. Express* **5**, 114–119 (1999).
- <sup>26</sup>J.-J. Zondy, A. Douillet, A. Tallet, E. Ressayre, and M. L. Berre, “Theory of self-phase-locked optical parametric oscillators,” *Phys. Rev. A* **63**, 023814 (2001).
- <sup>27</sup>A. Douillet, J.-J. Zondy, G. Santarelli, A. Makdissi, and C. Clairon, “A phase-locked frequency divide-by-3 optical parametric oscillator,” *IEEE Trans. Instrum. Meas.* **50**(2), 548–551 (2001).
- <sup>28</sup>D.-H. Lee, M. E. Klein, J.-P. Meyn, R. Wallenstein, P. Groß, and K.-J. Boller, “Phase-coherent all-optical frequency division by three,” *Phys. Rev. A* **67**, 013808 (2003).
- <sup>29</sup>Y. Jin, S. M. Cristescu, F. J. M. Harren and J. Mandon, “Femtosecond optical parametric oscillators toward real-time dual-comb spectroscopy,” *Appl. Phys. B* **119**(1), 65–74 (2015).
- <sup>30</sup>D. H. Jundt, “Temperature-dependent Sellmeier equation for the index of refraction,  $n_e$ , in congruent lithium niobate,” *Opt. Lett.* **22**, 1553–1555 (1997).
- <sup>31</sup>S. Zhang, W. You, X. Ma, M. Hu, and Q. Wang, “Spectral characteristics of femtosecond pulses propagation in periodically poled lithium niobate via cascaded quadratic nonlinearity,” *IEEE J. Quantum Electron.* **51**(5), 9000205 (2015).
- <sup>32</sup>R. DeSalvo, D. J. Hagan, M. Sheik-Bahae, G. Stegeman, E. W. Van Stryland, and H. Vanherzeele, “Self-focusing and self-defocusing by cascaded second-order effects in KTP” *Opt. Lett.* **17**(1), 28–30 (1992).
- <sup>33</sup>R. W. Boyd, S. G. Lukishova, and Y. R. Shen, *Self-focusing: Past and Present* (Springer, 2008).
- <sup>34</sup>C. R. Menyuk, R. Schiek, and L. Torner, “Solitary waves due to  $\chi^{(2)} : \chi^{(2)}$  cascading,” *J. Opt. Soc. Am. B* **11**(12), 2434–2443 (1994).
- <sup>35</sup>L. Torner, D. Mazilu, and D. Mihalache, “Walking solitons in quadratic nonlinear media,” *Phys. Rev. Lett.* **77**, 2455–2458 (1996).
- <sup>36</sup>T. Iizuka and Y. S. Kivshar, “Optical gap solitons in non-resonant quadratic media,” *Phys. Rev. E* **59**, 7148–7151 (1999).
- <sup>37</sup>K. Koynov and S. Saltiel, “Nonlinear phase shift via multi-step  $\chi^{(2)}$  cascading,” *Opt. Commun.* **152**, 96–100 (1998).
- <sup>38</sup>S. Saltiel and Y. Deyanova, “Polarization switching as a result of cascading of two simultaneously phase matched quadratic processes,” *Opt. Lett.* **24**, 1296–1298 (1999).

- <sup>39</sup>S. Saltiel, K. Koynov, Y. Deyanova, and Y. S. Kivshar, “Non-linear phase shift resulting from two-color multistep cascading,” J. Opt. Soc. Am. B **17**, 959–965 (2000).
- <sup>40</sup>S. T. Wong, T. Plettner, K. L. Vodopyanov, K. Urbanek, M. Digonnet, and R. L. Byer, “Self-phase-locked degenerate femtosecond optical parametric oscillator,” Opt. Lett. **33**, 1896–1898 (2008).
- <sup>41</sup>Z. Zhang, C. Gu, J. Sun, C. Wang, T. Gardiner, and D. T. Reid, “Asynchronous midinfrared ultrafast optical parametric oscillator for dual-comb spectroscopy,” Opt. Lett. **37**, 187–189 (2012).
- <sup>42</sup>A. V. Buryak, P. D. Trapani, D. V. Skryabin, S. Trillo, “Optical solitons due to quadratic nonlinearities: from basic physics to futuristic applications,” Phys. Rep. **370**, 63–235 (2002).
- <sup>43</sup>M. Marangoni, C. Manzoni, R. Ramponi, and G. Cerullo, “Group-velocity control by quadratic nonlinear interactions,” Opt. Lett. **31**, 534–536 (2006).
- <sup>44</sup>W. Lu, Y. Chen, L. Miu, X. Chen, Y. Xia, and X. Zeng, “All-optical tunable group-velocity control of femtosecond pulse by quadratic nonlinear cascading interactions,” Opt. Express **16**, 355–361 (2008).
- <sup>45</sup>J. -C. Diels, and W. Rudolph, *Ultrashort Laser Pulse Phenomena* (Elsevier, 2006).